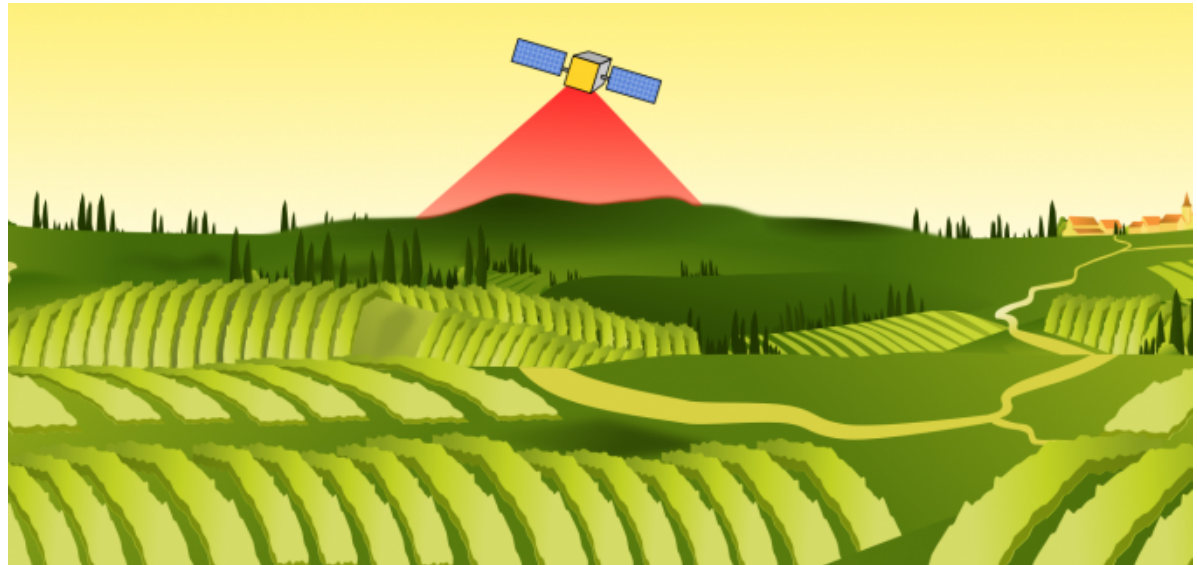# Applications of SAR for Agriculture

What Applications?

- Crop type
- Land use change
- Crop condition
- Leaf Area Index and biomass
- Crop phenology

- Soil moisture

Image source: gisgeography.com/farming-agriculture-technology/

Crop Identification

- traditionally accomplished using optical data
- when available at the right time in the growing season, optical data does very well
- but….

crop type

2010

Edmonton

0 25 50 100 km
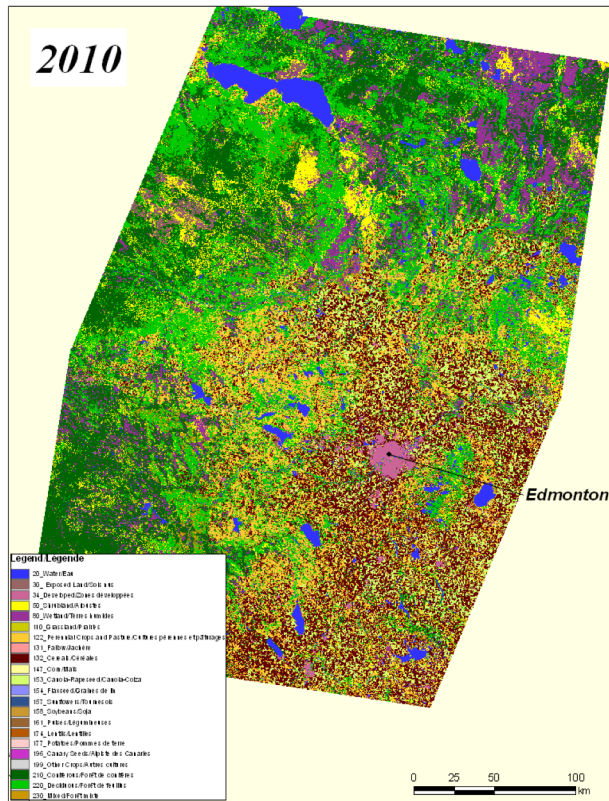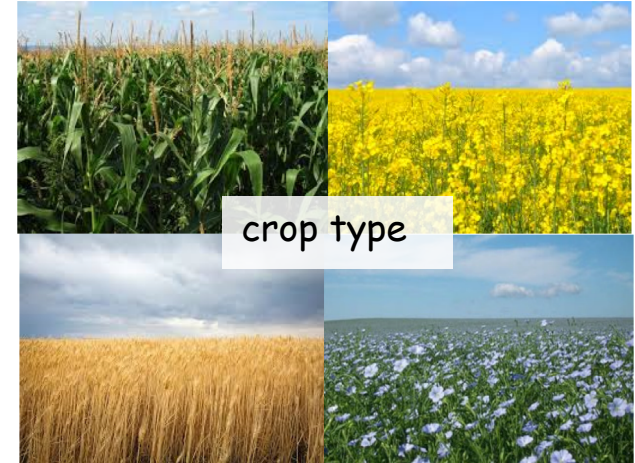
Optical + Single Frequency SAR (Edmonton, Canada)

Landsat 5:

2010-06-20

RADARSAT-2:

2010-05-28

2010-06-21

2010-07-15

2010-08-08

Overall accuracy

- with Landsat only (< 70%)
- including ScanSAR Narrow (VV, VH) data (89.1%)

3

Image source: Agro-climate, Geospatial and Earth Observation group, Agriculture and Agri-Food Canada

Crop Identification

Rule Number 1: Make sure you collect the right type of data

Polarization:

- #1: **HV or VH**. The cross-polarization responds to volume scattering in the crop canopy and the amount of volume scattering is crop-type specific

- #2: **VV**. The vertically-oriented waves couple with vertical structures which either scatter or attenuate signal.

- Last: HH-polarization: usually the least helpful but can assist with separating some crops (like forages)

- Bottom line: VV-VH is the best dual polarization combination

VH/HV + VV

Crop Identification

Frequency

- more difficult to determine as we want some penetration into the canopy, but not too much
- difficult because penetration depends on canopy volume and this changes for different crops and different growth stages
- ideally a multi-frequency approach (X+C, C+L, X+C+L), which provides excellent results
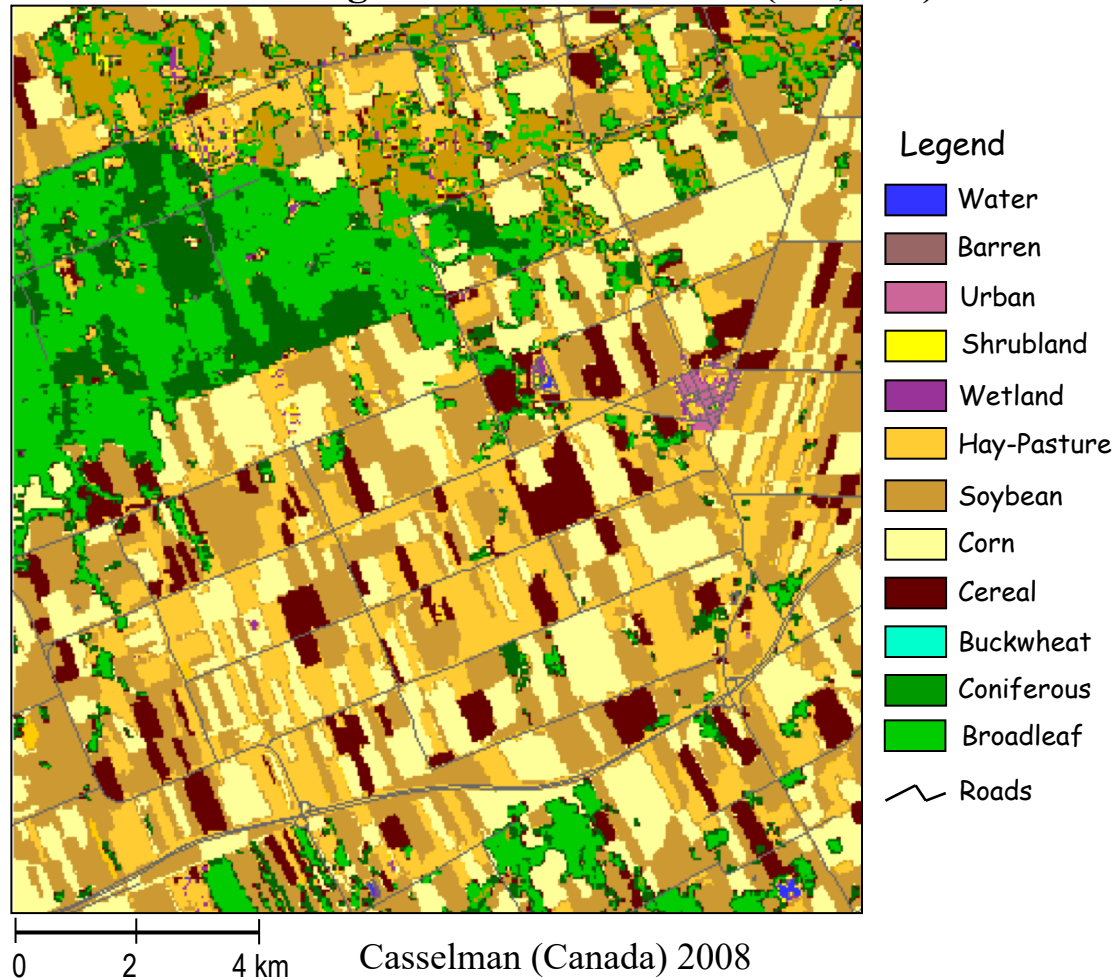
Multi-temporal

- as with optical approaches, multi-temporal data are critical
- crops may look very similar to SAR at one growth stage, but very different at another
- generally, the single best time for crop separation is when crops are in their **seed development/reproductive** stage. An acquisition at this time is important because this is when crop structure changes the most

Single Frequency Multi-polarization SAR

In general, classification is best with higher frequencies (shorter wavelengths) as this provides best opportunity for multiple scattering within the canopy

Classification using 6-date TerraSAR-X (VV, VH)

Legend
- Water
- Barren
- Urban
- Shrubland
- Wetland
- Hay-Pasture
- Soybean
- Corn
- Cereal
- Buckwheat
- Coniferous
- Broadleaf
- Roads

0   2   4 km

Casselman (Canada) 2008

X-Band provides excellent classification results

Still, best option is multi-frequency

X-Band = 84.9% (6 images)
C-Band = 75.4% (4 images)
X + C = 87.3%

Integrating Multiple Frequencies

X-, C- and L- Band: Carman 2009

CFIA (2006) (corn, soybean, wheat, forage/hay): **C- and L-Band 82.9%**
Casselman (2008) (corn, soybean, wheat, forage/hay): **X- and C-Band 87.3%**
Carman (2009) (canola, flax, beans, corn, cereals): **X, - C- and L-Band: 91.4%**

Early Season Crop Identification

End of season TerraSAR-X crop classification: Ottawa 2012
Overall accuracy: **97.2**%

Early season: Corn can be identified at V6 or 6th leaf collar stage (about 6 weeks after planting)

N

Kilometers
0 0.75 1.5   3

Roads

Water

Forest and other permanent vegetation

Developed

Pasture-Forage

Corn

Soybean

Information source: McNairn et al. (2014)
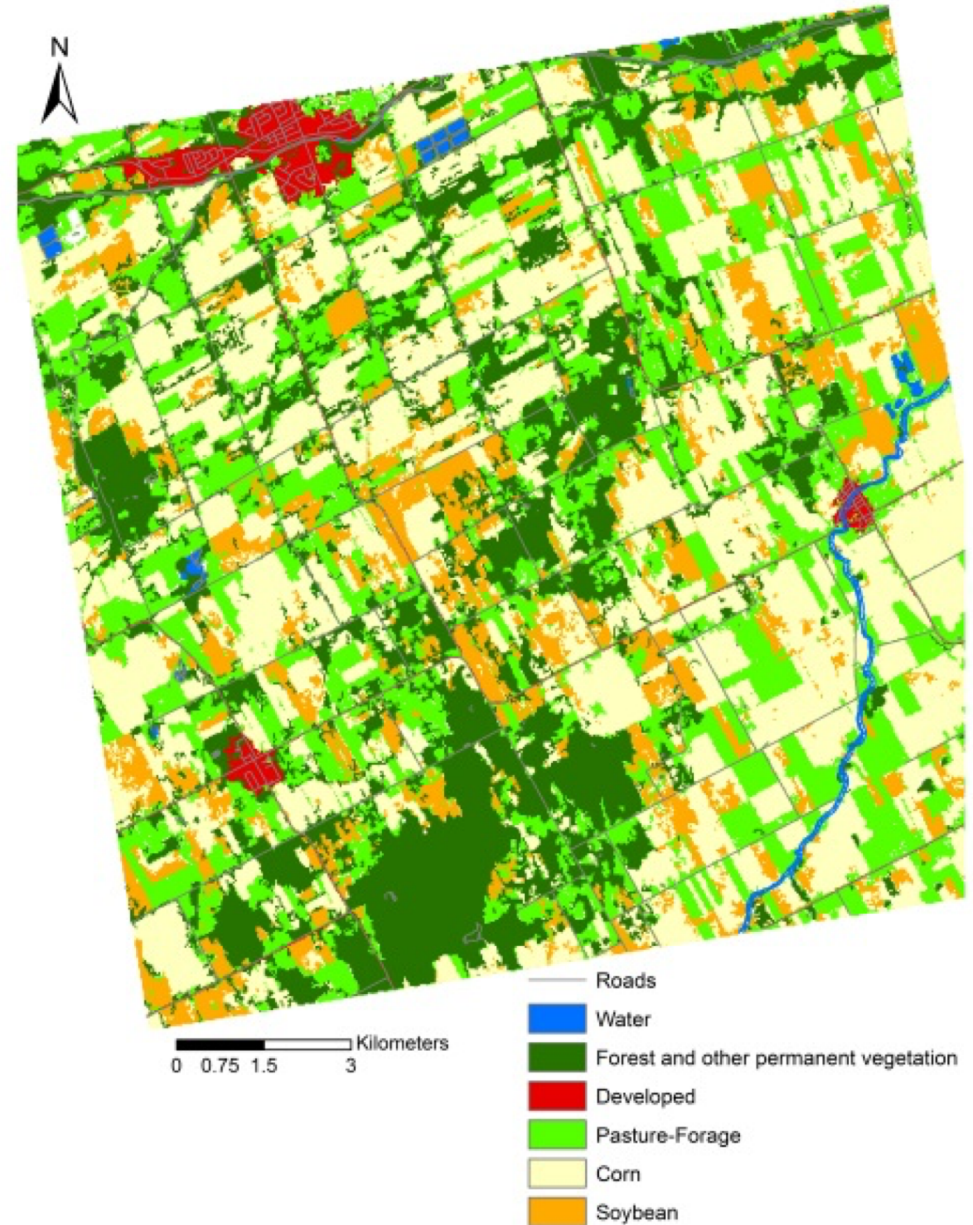
What About Fully Polarimetric?

- some sensors offer fully polarimetric modes

- these modes allow users to synthesize many radar parameters in addition to HH, HV/VH and VV

- provide better accuracies than dual-polarizations

RADARSAT-2 Indian Head 2009

Producer's accuracies

Class	Linear intensity	Cloude decomposition
Pasture/forage	77.8	**81.2**
Fallow	40.7	**73.1**
Canola	95.3	95.4
Flaxseed	23.1	41.6
Lentils	80.9	**95.3**
Field peas	97.2	97.1
Cereals	97.7	97.8
Overall	87.2	89.0

RADARSAT-2 (June 15, July 6, August 9, September 2): Casselman 2008

Dates of Data Acquisition	User's Accuracy				Producer's Accuracy				
	Pasture	Soy	Corn	Wheat	Pasture	Soy	Corn	Wheat	Overall
Cloude-Pottier (E, A, α)	77.5	85.2	86.4	97.6	80.6	87.4	86.8	84.9	85.8
Freeman-Durden	85.1	93.7	89.9	93.3	85.7	92.4	94.5	83.4	**90.9**
Linear Polarizations (HH, HV, VV, VH)	60.4	81.8	73.6	83.8	66.2	82.9	76.1	64.0	75.4

…And Compact Polarimetry?

wetland
water
forest
developed
pasture
soybean
corn
cereals
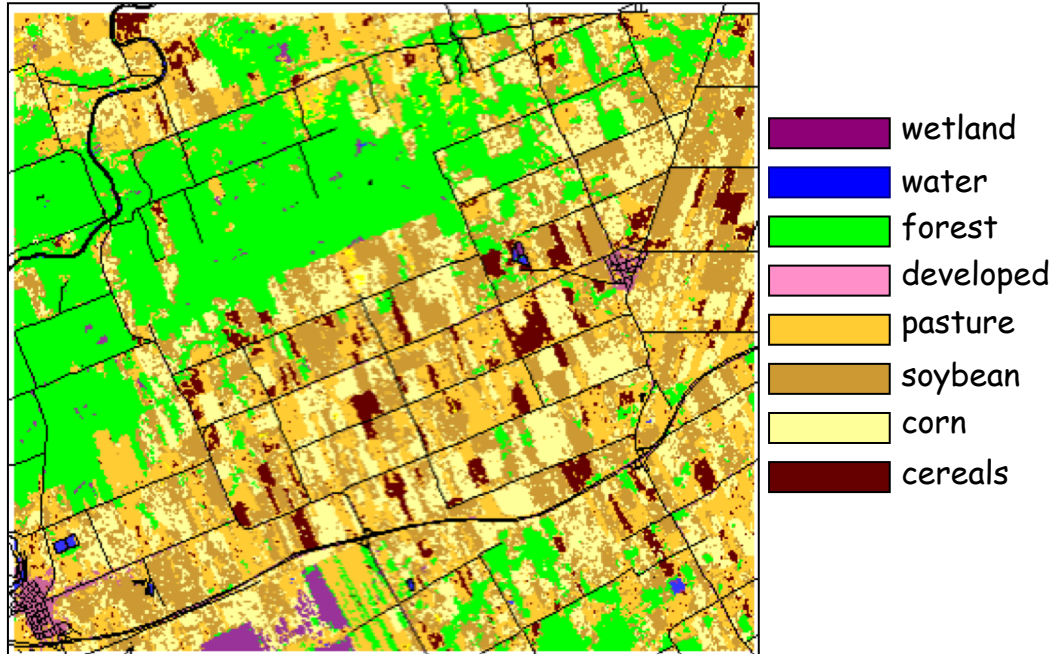
Classification generated from mDelta

mDelta: single, double, volume

84.3% overall accuracy

- compact Polarimetry lies in world between multi-polarization and full polarimetry

- CP can be implemented for wide swaths and is thus of significant interest for regional and national monitoring

- RADARSAT Constellation Mission (RCM) and SAOCOM-1A also have CP capabilities.

- CP parameters outperformed dual polarizations (results from 2008 and 2010)
  - small improvements in overall accuracies (1.5 to 2.7%)
  - larger improvements in individual dates (up to 21.5%)
  - large increase in accuracy for wheat (10.2% (producer's) to 11.4 (user's) for 2010)
  - smaller gains in other classes (<3%)

SAR Was "Born" to Monitor Rice

Backscatter from Land Cover Classes in Zhao Qing, China

Double-bounce scattering for flooded rice paddies
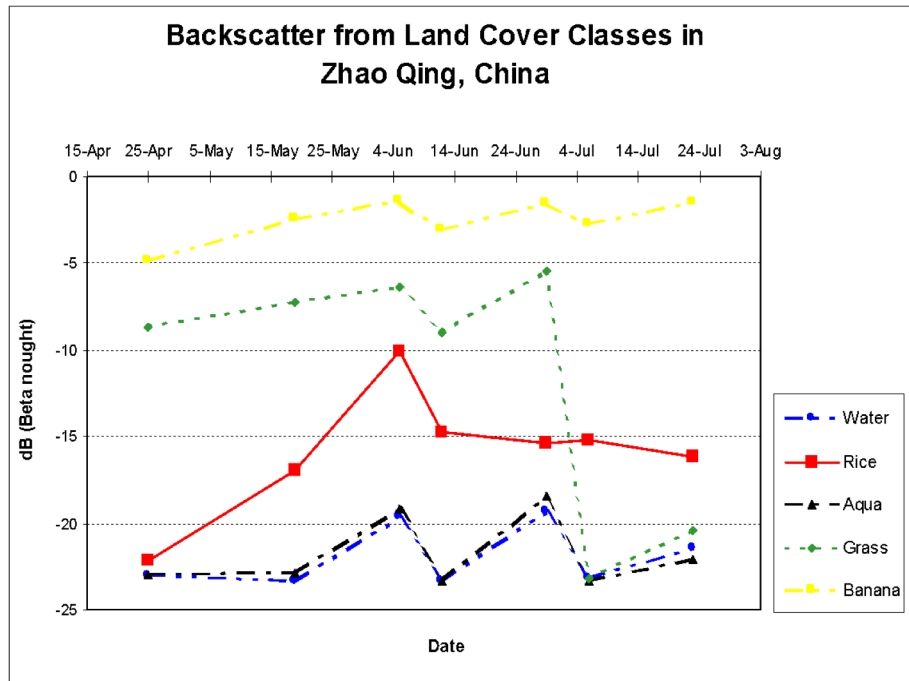
- 12 dB change in **rice** areas from beginning of growing season to peak growing season

- **Banana** target consistently bright

- **Grass** provided constant return of -5 to -8 dB, until flooded mid-season

- **Water** and aquaculture consistently dark between -19 and -24 dB

Rice Monitoring: The Philippines

Rice Fields

Timing of Planting

■ Before June 11	■ June 11 – June 23	■ June 23 – July 05	■ July 05 – July 17
■ July 17 – July 29	■ July 29 – August 10	■ After August 10	
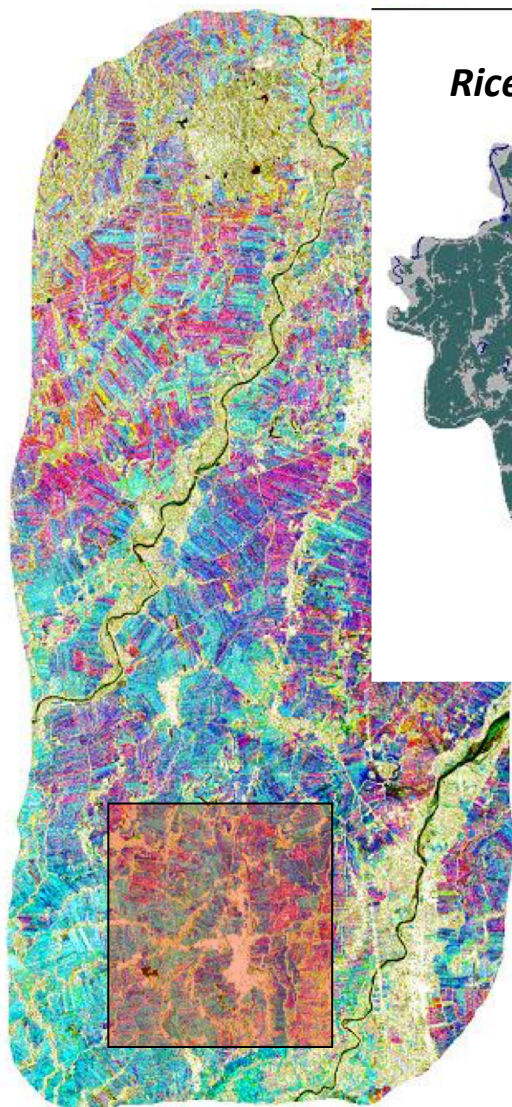
Multi-date RADARSAT-1
Santo Domingo
The Philippines (2001)

■ 1000 – 2000 kg/ha	■ 2000 – 3000 kg/ha	■ 3000 – 4000 kg/ha	■ 4000 – 5000 kg/ha
■ 5000 – 6000 kg/ha	■ 6000 – 7000 kg/ha	■ 7000 – 8000 kg/ha	

Rice Yields

12

Information source: Chen and McNairn (2006)
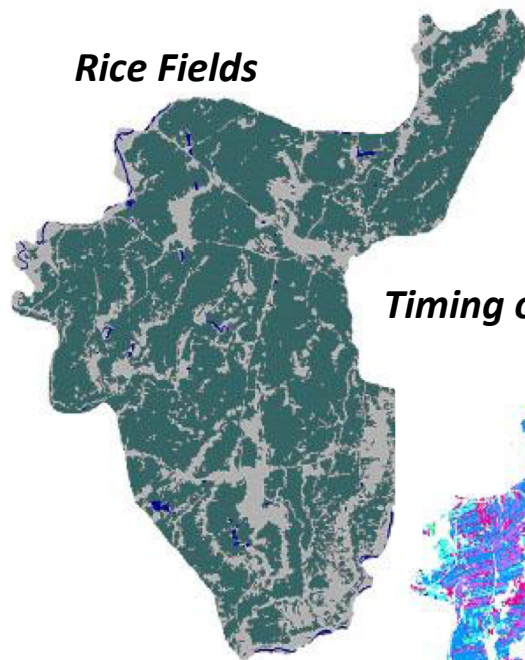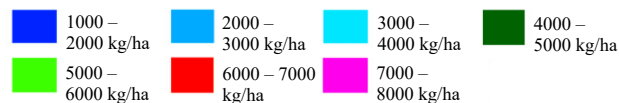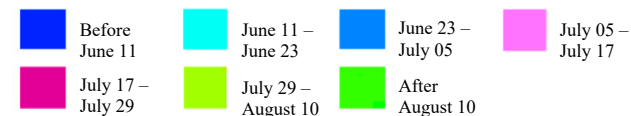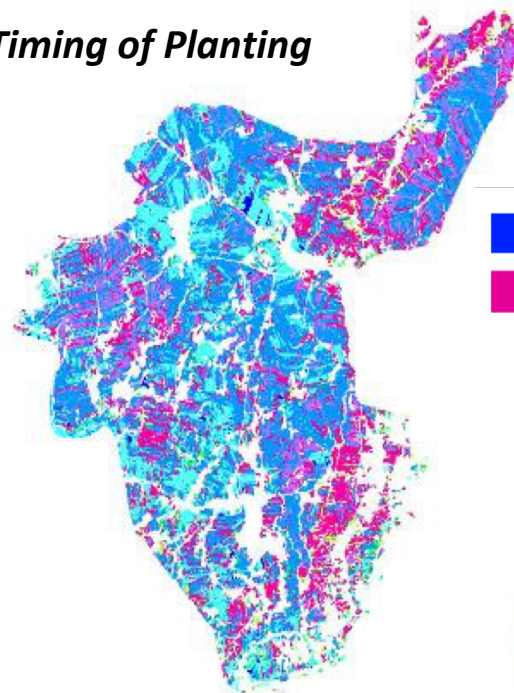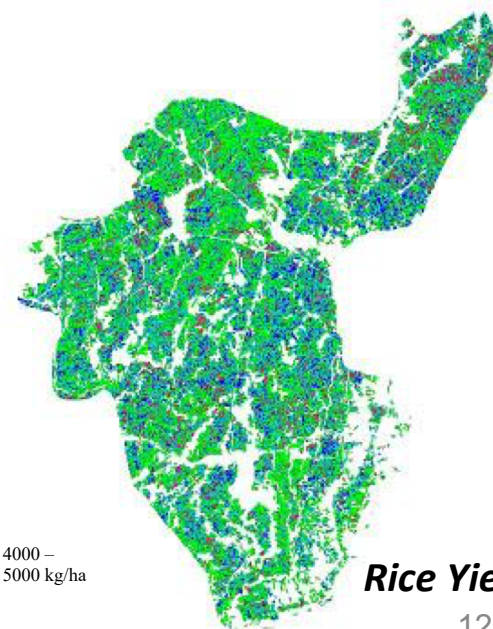
Land Use Change

Rice Monitoring with TerraSAR-X
Xuwen, China

	Rice planted	No rice planted
🟥	2008	2009
🟩	2009	2008
⬛	2008, 2009	
⬜		2008, 2009
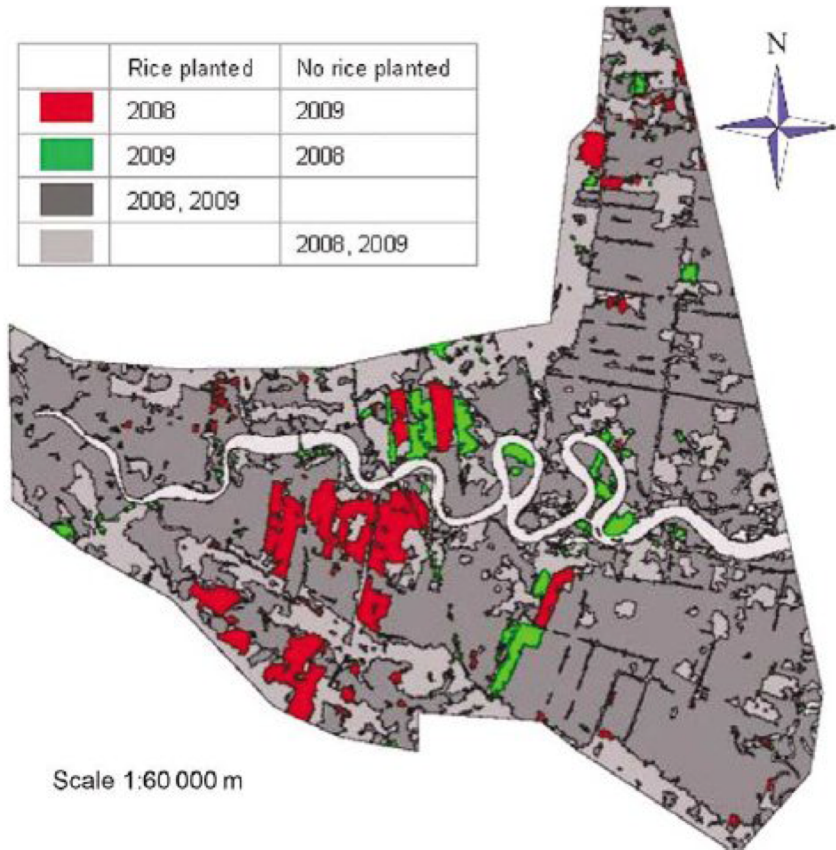
- Almost 15 000 ha of rice was under cultivation in the Xuwen study site

- 10% of this land experienced change (rice to non-rice or non-rice to rice)

- Changes driven by market demand as prices of other cash crops (peanut and watermelon) were high spurring farmers to drain rice paddies to plant cash crops.

Scale 1:60 000 m

Red: Paddies planted in rice in 2008 but not 2009
Green: planted in rice in 2009 but not 2008
Dark grey: planted in rice both years
Light grey: non-rice fields

Information source: Pei et al. (2011)

13

Crop Condition

- SAR responds to changes in structure and changes in moisture
- this can be exploited to inform on condition of crops
- traditionally done using optical data, including optical indices
- optically, cloud-cover is dealt with by integrating data in time to create 7- or 10-day mosaics

- **Question** : Can SARs be used to provide information on crop condition to fill gaps and provide crop condition information at field scales?
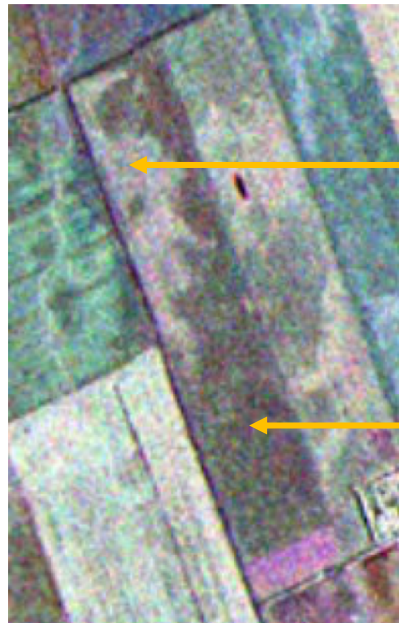
crop condition

Barley
Poor growth affected by N losses due to poor soil drainage

Barley
Healthy growth

Airborne SAR (VV, VH, HH)
June 28, 2000
Indian Head, SK

Crop Condition - SAR Classification using Linear and Circular Polarizations

Good growth, but with significant weed infestations

Poorer growth

Poorer growth

Vigorous growth

K-means unsupervised classification using 7 SAR polarizations (RR, RL, HH, VV, HV, ψ = 45° and 135°)

Moderate growth

Poorer growth

Vigorous growth

Moderate growth

Yield vs SAR

Area of Agreement (Higher Yield)
Area of Agreement (Lower Yield)] 77%
"Error" (omission/comission) 23%
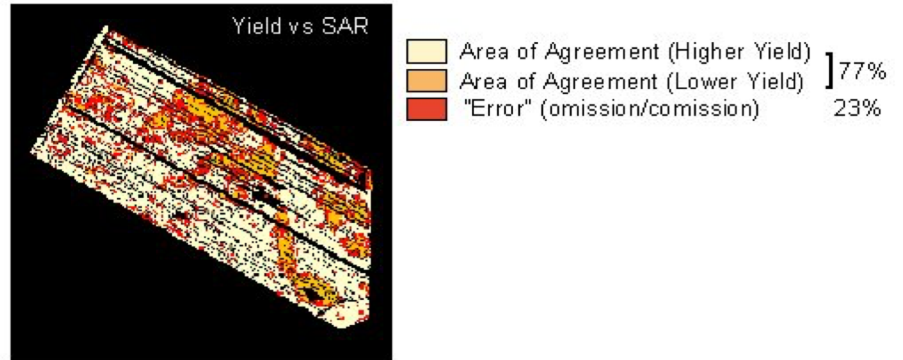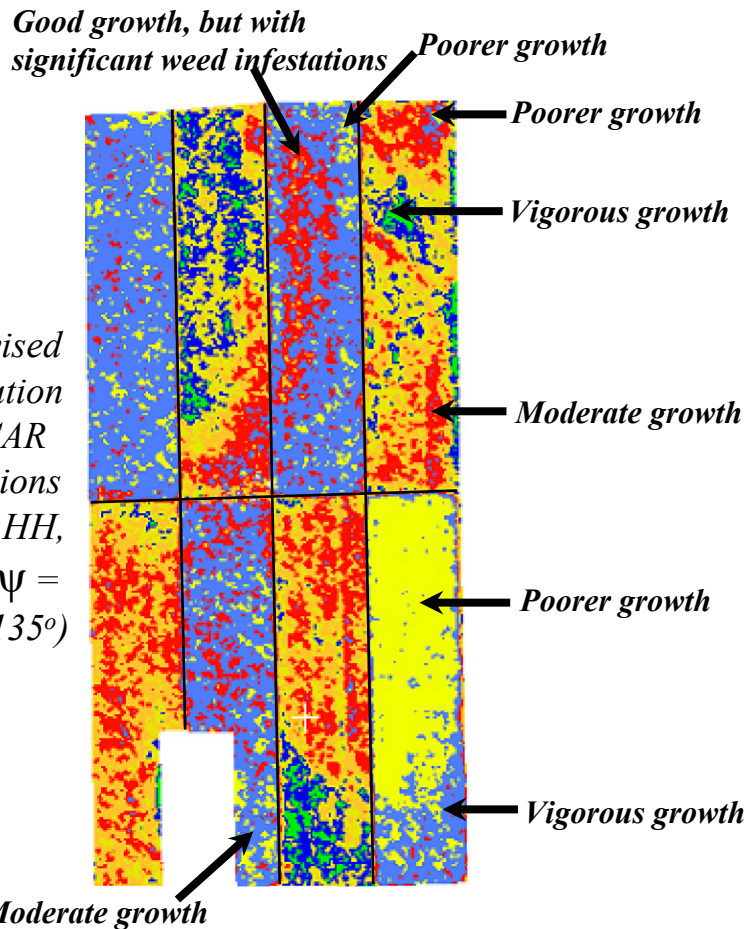
A classified image of a wheat fields was generated using HH, VV and HV polarizations from CV-580 data acquired over Clinton, Ontario (Canada) on June 30, 1999.

These classes were then compared to classes generated from crop yield monitor data (bushels per acre).

A good relationship was established between regions of high and low yield and radar response.

Crop Condition - Pedestal Height

Co-polarization pedestal height
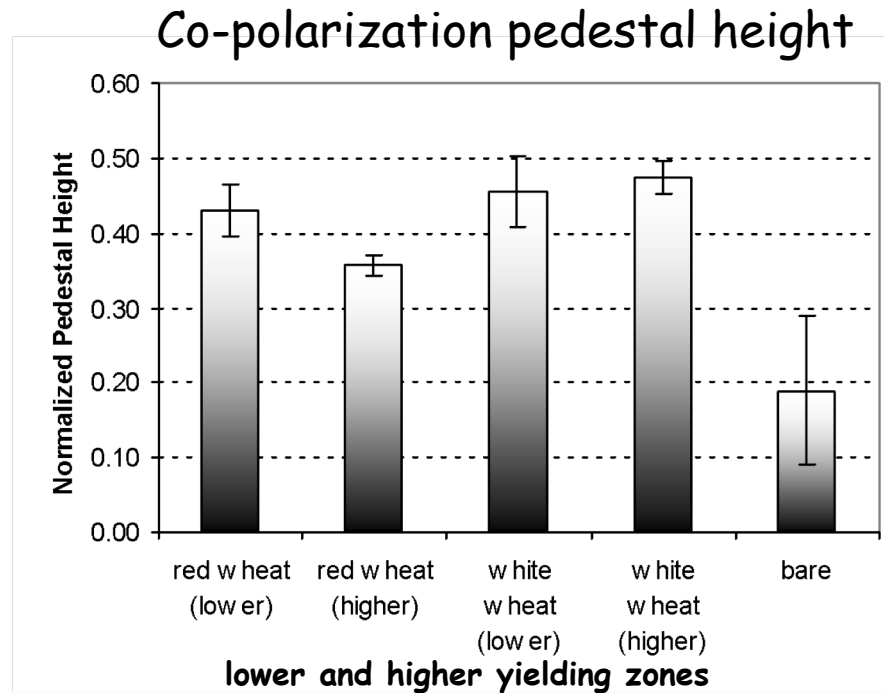
• co-polarization pedestal height is larger for the cropped (wheat) fields relative to the bare field

• the low pedestal height for the bare field is typical of surface scatterers where the degree of polarization is high

Crop Condition and Productivity

Corn and Soybean Productivity (LAI and Biomass)
Using RapidEye Satellite
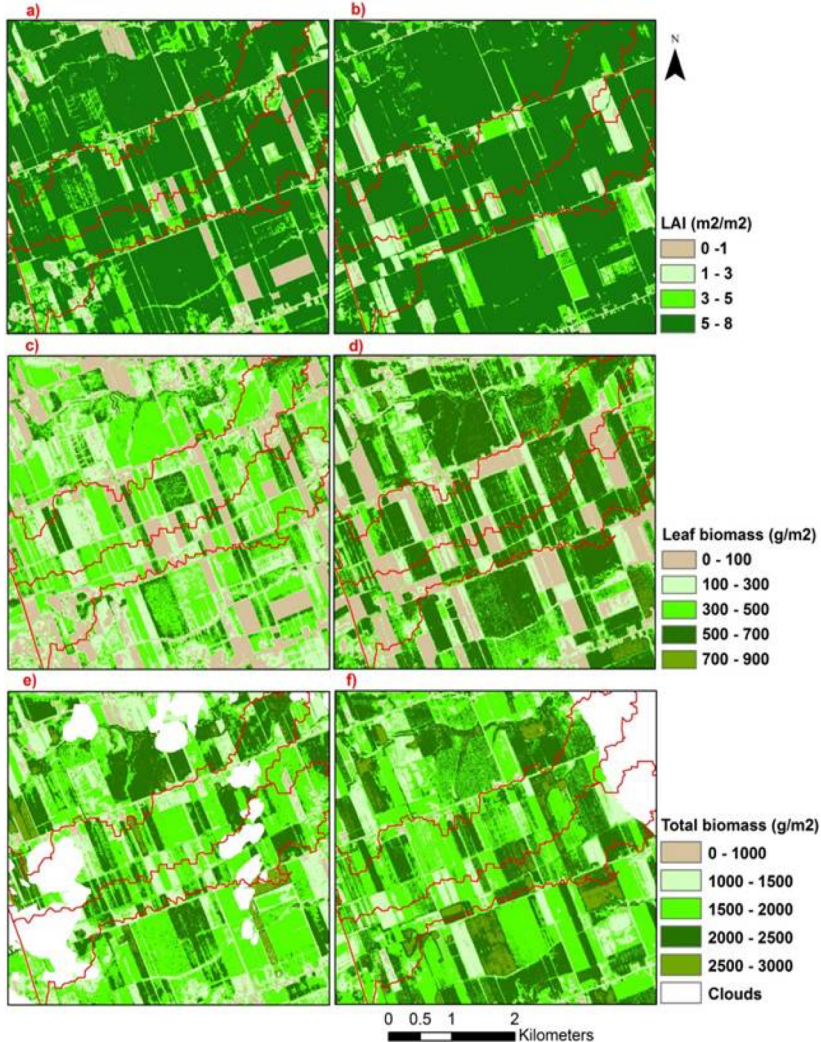
2012 (very dry year)   2013 (very wet year)

- Leaf Area Index and biomass are strong indicators of productivity and can be linked through process models to crop yield

- these indicators can be assimilated into crop growth models to improve model estimates (of yield, biomass etc.). However, operationally, data must be delivered consistently especially in the rapid early stages of crop growth

- there is a strong statistical relationship between backscatter and LAI/biomass

- **Note**: SAR parameters affected by volume scattering are, by far, most sensitive to crop condition:

  - HV or VH intensity (backscatter)

  - volume scattering components of SAR decompositions

  - indicators of unpolarized and random scattering (such as entropy)

Information source: Kross et al. (2015)

17

How Are LAI and Biomass Estimated from SAR?

- several modelling approaches, each with advantages and disadvantages
  - empirical
  - semi-empirical
  - physical

SAR modelling with Water Cloud Model (Semi-Empirical)

$$\sigma^0 = AL^E \cos\theta (1 - \exp(-2BL/\cos\theta)) + \sigma_{soi}^0 \exp(-2BL/\cos\theta)$$

Total backscattered by the whole canopy (σ^o) at incidence angle (θ)

$$\sigma_{veg}^0 = AL^E \cos\theta (1 - \tau^2)$$

$$\tau^2 = \exp(-2BL/\cos\theta)$$

Vegetation component

$$\sigma_{soil}^0 = C + DM_s$$

Soil component

t^2 is the two-way attenuation through the canopy layer
L is the LAI or biomass (expressed in m^2/m^2 or g/m^2)
A,B,C,D and E are model coefficients defined by experimental data (A,B, E depend on canopy type)

18

Leaf Area Index from RADARSAT-2

June 16, 2012

July 10, 2012

August 6, 2012

August 30, 2012
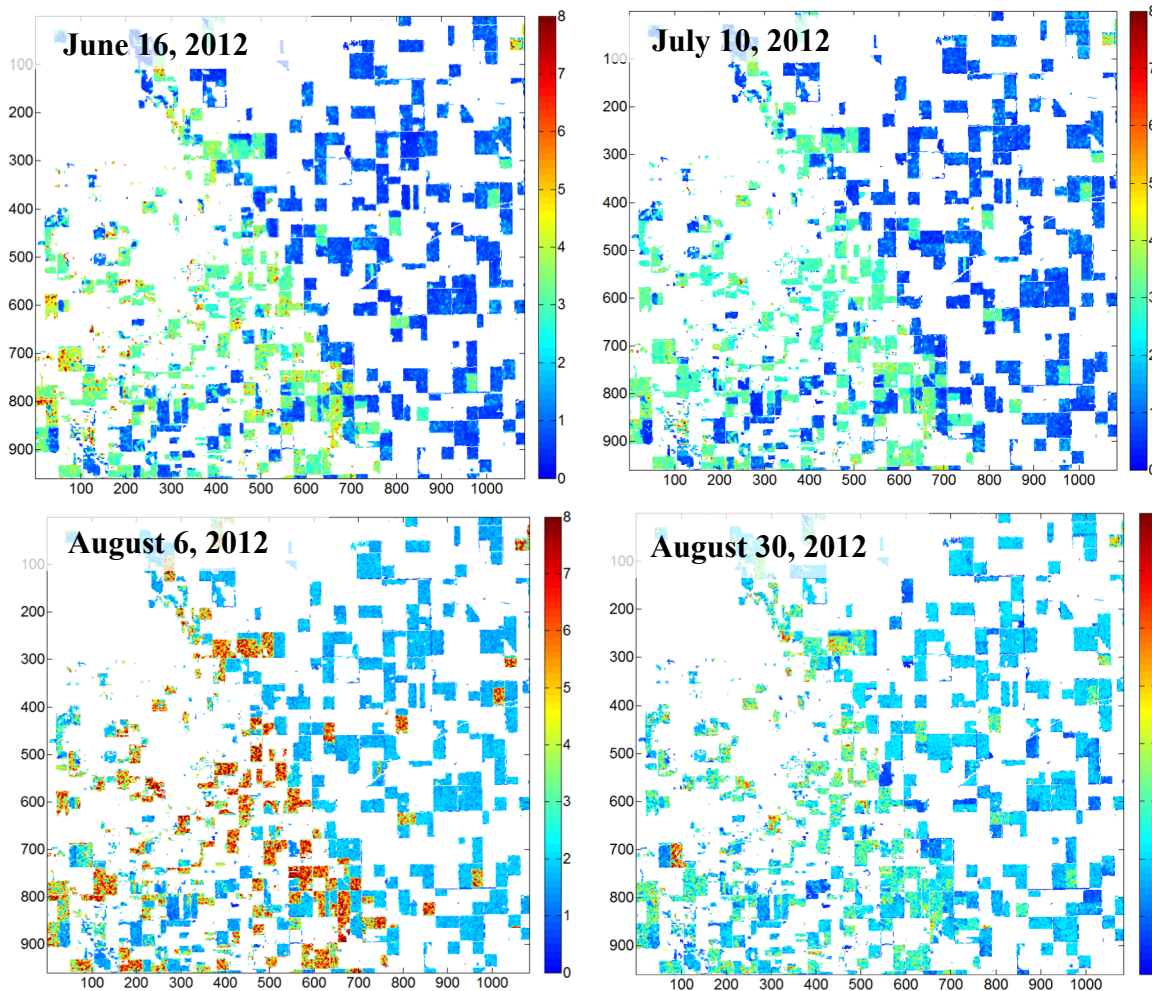
Manitoba, 2012

LAI and biomass estimates for corn, soybeans and wheat

Accuracies with C- and L-band similar (or better than) than accuracies using optical data
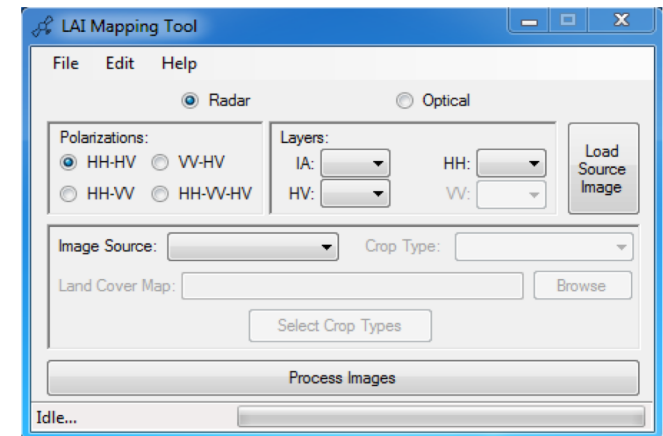
			R
Corn HH-HV	0.84	0.65	0.83
Corn VV-HV	0.75	0.62	0.81
Soybeans HH-HV	0.64	0.44	0.80
SoybeansVV-HV	0.63	0.44	0.80

Information source: Hosseini et al. (2015)

19

Estimating Crop Biomass from RADARSAT-2
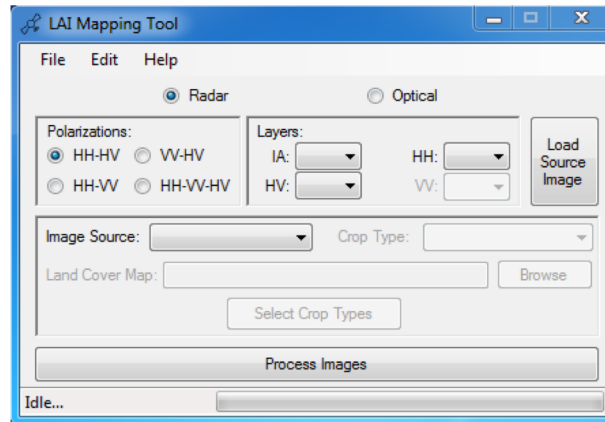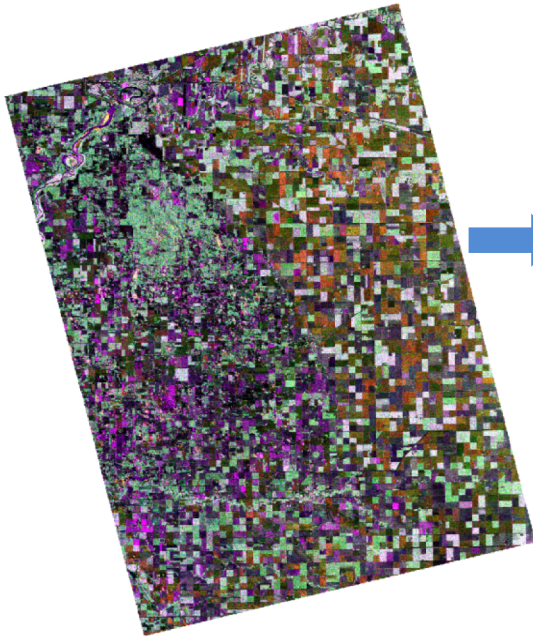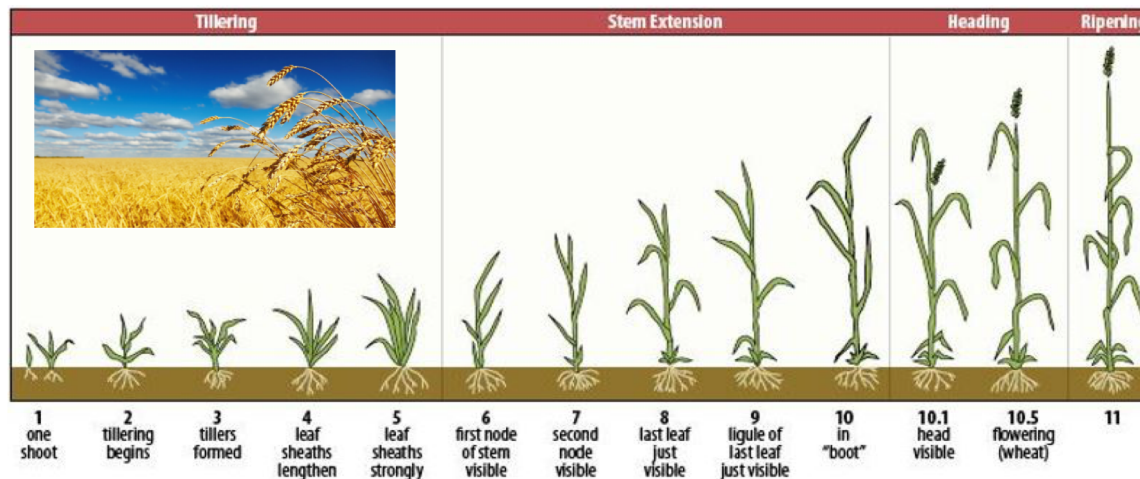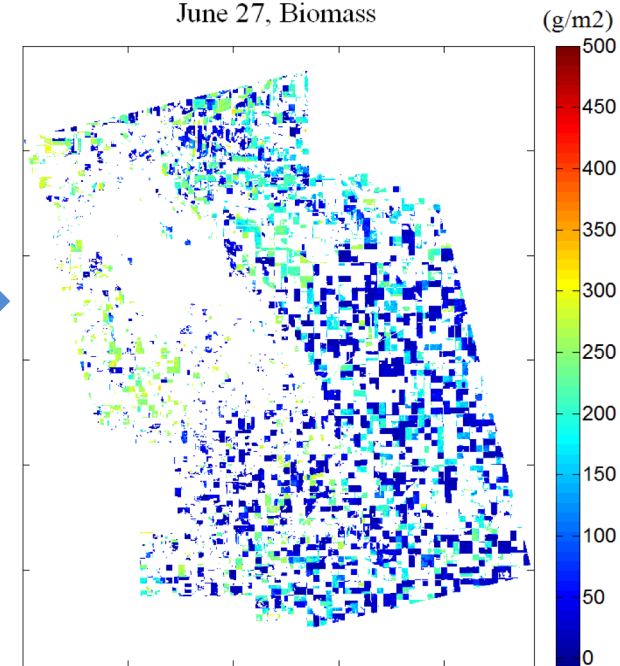
Forecasting Crop Phenology using Machine Learning

Carman Canola field--Can09
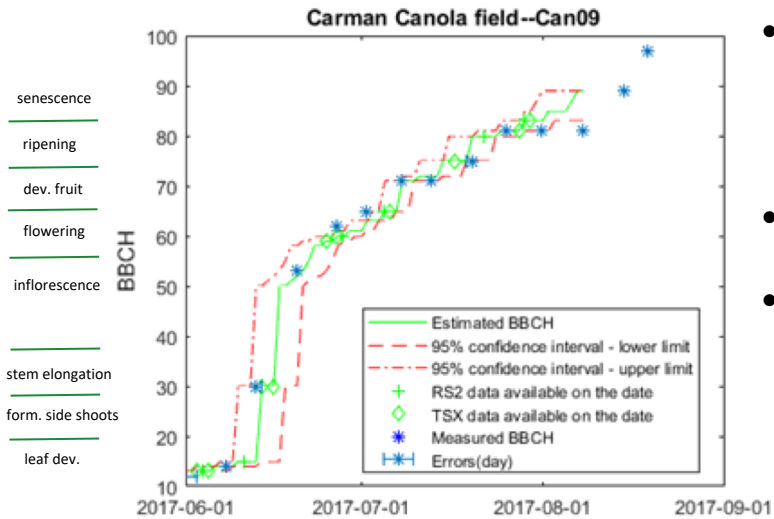
- AAFC collaborated with A.U.G. Signals who developed a machine learning algorithm to identify and forecast crop growth stage (BBCH scale), on a daily time step

- Input data are RADARSAT-2 and TerraSAR-X imagery

- The machine learning algorithm updates existing estimates of growth stages and improves forecasts as new data become available

Estimated and Ground measured BBCH(Carman MB)

Yellow fields identified as canola fields in bloom

Airborne Underwater Geophysical Signals

Information source: McNairn et al. (2018)
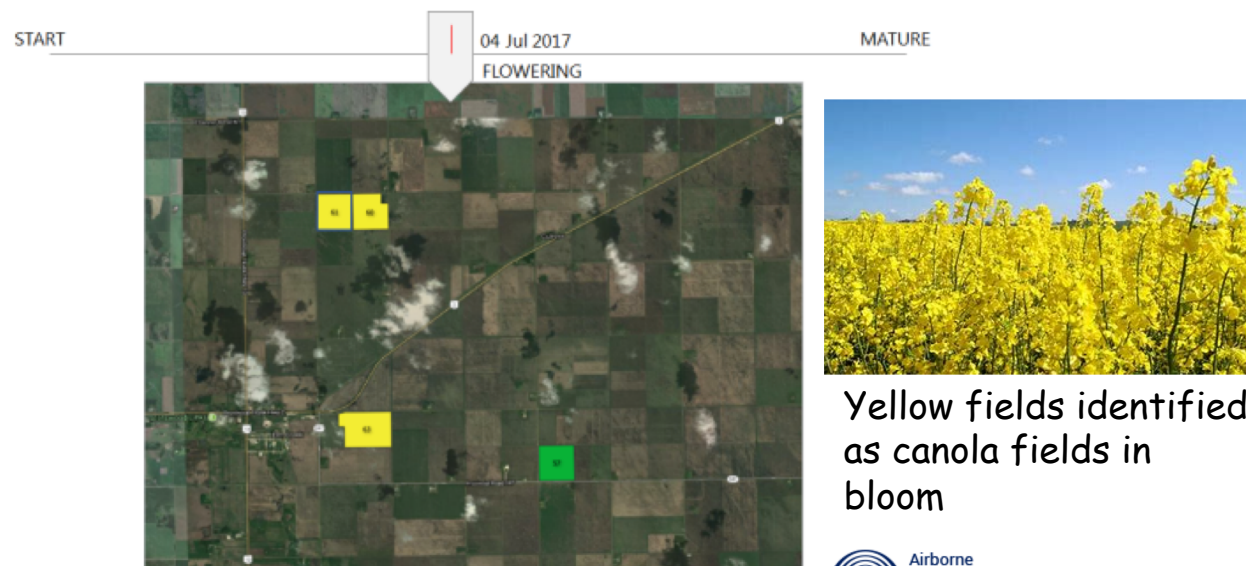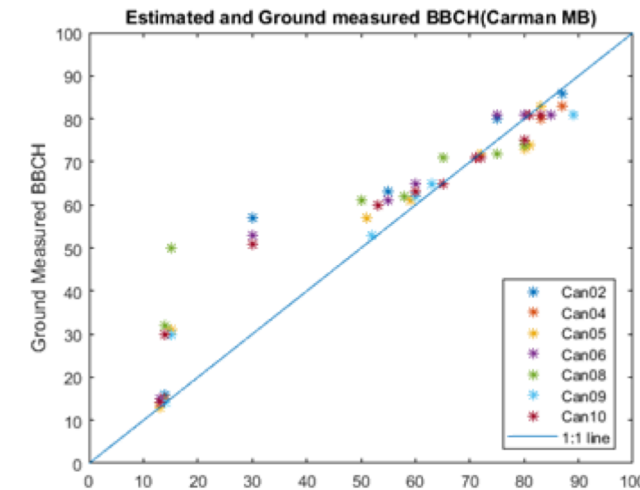
Methods to Estimate Soil Moisture

Empirical models
- simplest approach and models are easy to invert
- requires extensive field data and statistical models are usually not robust

Change detection
- easy to apply
- assumes that soil moisture changes over time but that roughness changes are small
- relies on good relative calibration and images must all be acquired using the exact same radar configuration (only moisture changes)
- provides only relative changes, unless change is calibrated with ground data

Semi-empirical models (such as Oh or Dubois models)
- more robust than empirical, but coefficients may not always be valid under new circumstances
- have specific ranges of validity upon which models were developed
- relatively easy to invert

Physical scattering models (such as the Integral Equation Model)
- model scattering behaviour
- also have a range of validity
- complex to invert

How Do I Start?

Rule Number 1: Make sure you collect the right type of data

- **Frequency**
  - longer wavelengths are preferred
  - greater penetration
  - reduces roughness effects

- **Polarization**
  - a polarization that responds to surface scatter (HH or VV) is preferred
  - semi-empicial and physical models will require specific polarizations

- **Incident angles**
  - empirical approaches: stick to steep angles where roughness effects are reduced
  - semi-empirical or physically modelling: angle is parameterized in model so choice is less critical
  - change detection: very important to stick with same repeat angle

Empirical Models

© 2004 Canadian Space Agency

Sensitivity of HH Backscatter to Surface Soil Moisture

HH = -12.12 + .07797 * Soil Moisture
r = 0.857

HH Backscatter (dB)

Percent Surface Volumetric Soil Moisture (0-2.5 cm)
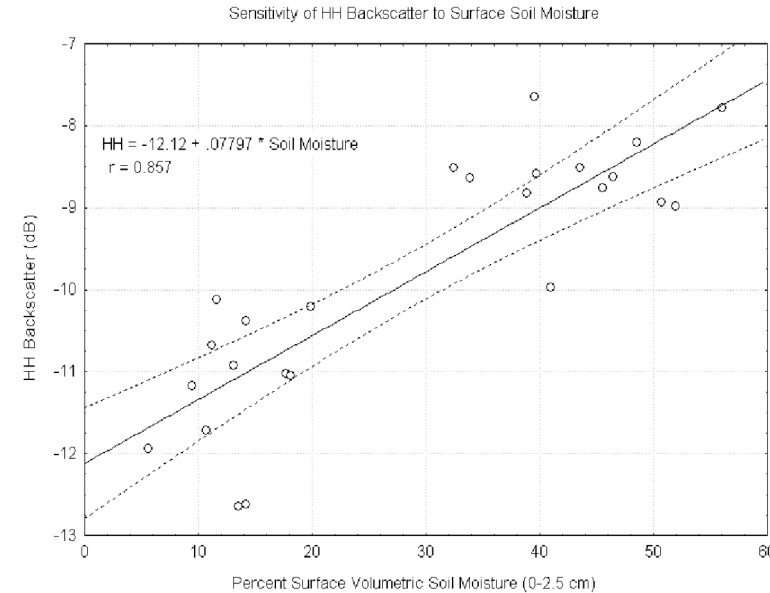
• a statistical model is developed based on the regression of volumetric soil moisture against radar backscatter

• regression coefficients developed from field measurements

• model is then inverted to predict soil moisture across the entire image

■	Unclassified
■	1 to 10 %
■	10 to 20 %
■	20 to 30 %
■	30 to 40 %
■	40 to 50 %
□	Over estimated

ALTONA

Imagery provided by the Canada Centre for Remote Sensing

Soil moisture = -12.96 +(3.158 * incidence angle) + (8.772 * C-HH)
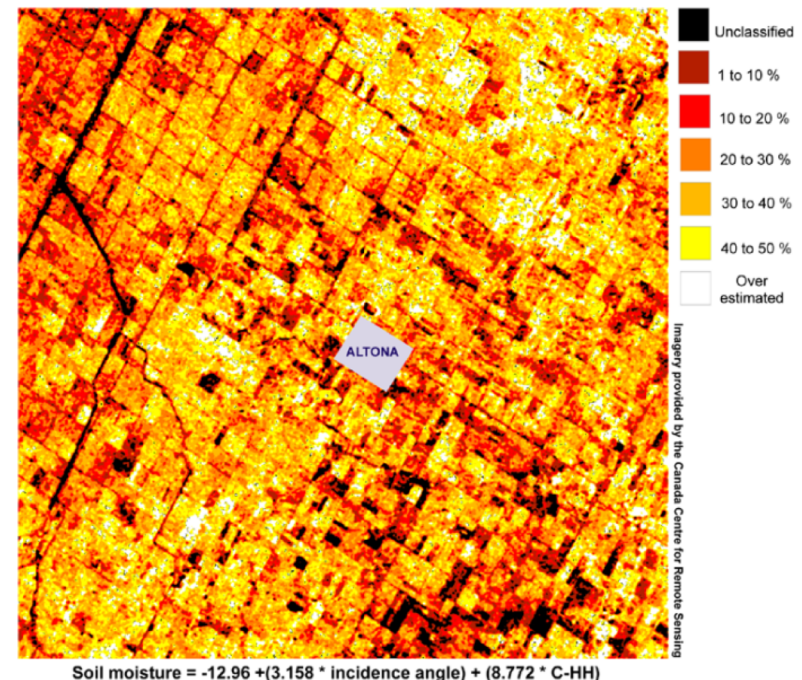
Change Detection

S1 Ascending 25-September-2004

© 2004 Canadian Space Agency
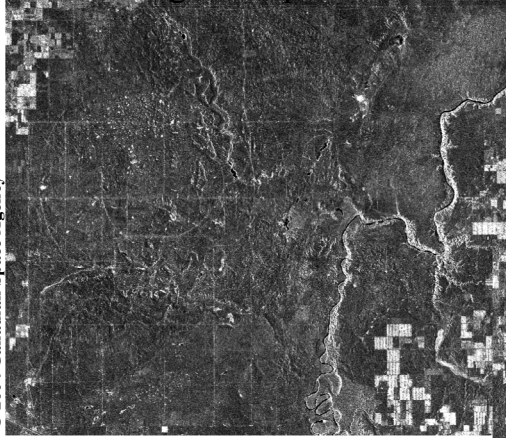
No rain 7 days
prior to acquisition

S1 Ascending 19-October-2004

© 2004 Canadian Space Agency
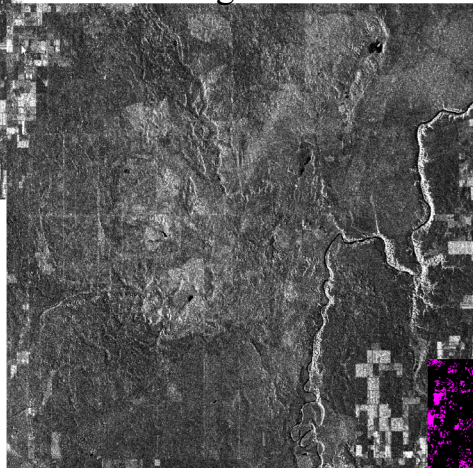
Rain day
before acquisition

Both S1 Ascending
RADARSAT images acquired
24 days apart

Change Image
Threshold of 7dB

Change Image
Threshold of 5dB

Colour identifies
areas of significant
change in soil
moisture in this 24-
day period

Semi-empirical Models

- backscatter is related to sensor (frequency, incidence angle, polarization) and target (dielectric and random roughness) characteristics
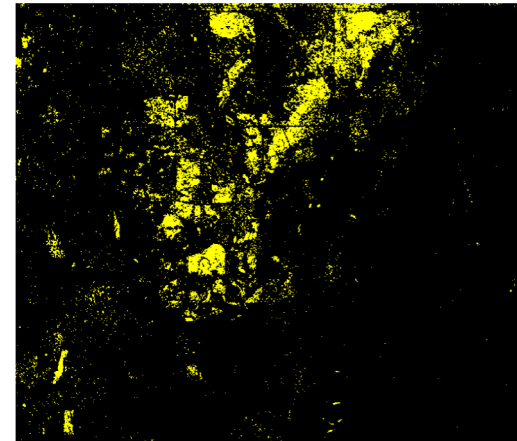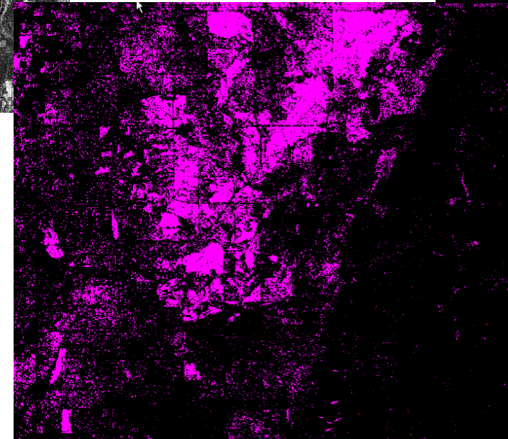
- models mathematically relate backscatter to these variables

- coefficients are derived from extensive field work (often using scatterometer measurements)

- most models relate soil, incidence angle and frequency characteristics to backscatter at a single polarization or polarization ratio

- sensor parameters are known and two equations are solved iteratively for either dielectric or roughness

- models include one roughness variable - rms (correlation length is usually ignored)

- dielectric mixing models are related to derive volumetric soil moisture for dielectric

Semi-empirical Models

Oh Model

$$\alpha = \sigma^o_{hh}/\sigma^o_{vv} = [1 - (2\theta/\pi)^{1/3\,\Gamma_0} \exp(-ks)]^2$$

$$\beta = \sigma^o_{hv}/\sigma^o_{vv} = 0.23\sqrt{\Gamma_o}(1 - \exp(-ks))$$

$$\Gamma_h = \left| \frac{\cos\theta - \sqrt{\varepsilon_r - \sin^2\theta}}{\cos\theta + \sqrt{\varepsilon_r - \sin^2\theta}} \right|^2$$

$$\Gamma_v = \left| \frac{\varepsilon_r \cos\theta - \sqrt{\varepsilon_r - \sin^2\theta}}{\varepsilon_r \cos\theta + \sqrt{\varepsilon_r - \sin^2\theta}} \right|^2$$

$$\Gamma_o = \left| \frac{1 - \sqrt{\varepsilon_r}}{1 + \sqrt{\varepsilon_r}} \right|^2$$

σ^o = backscatter (sigma)
θ = incidence angle (radians)
εr = real part of the dielectric constant
k = is the wave number (k=2π/λ)
s = root mean square height (cm)

Dubois Model

$$\sigma^o_{hh} = 10^{-2.75}(\cos^{1.5}\theta/\sin^5\theta)10^{0.028\varepsilon_r \tan\theta}(ks\sin\theta)^{1.4}\lambda^{0.7}$$

$$\sigma^o_{vv} = 10^{-2.35}(\cos^3\theta/\sin^3\theta)10^{0.046\varepsilon_r \tan\theta}(ks\sin\theta)^{1.1}\lambda^{0.7}$$

λ = wavelength (cm)
σ^o = backscatter (sigma)
θ = incidence angle (radians)
εr = real part of the dielectric constant
k = is the wave number (k=2π/λ)
s = root mean square height (cm)

Integral Equation Model - IEM

- Integral Equation Model (IEM): a model adapted to randomly dielectric rough surfaces to simulate the backscattering behaviour for the wide range of surface roughness values.

- 3 unknowns: rms, correlation length, dielectric → requires 3 measures of backscatter

- a calibrated version of IEM is available: reduces the model parametrization from three unknowns (dielectric constant; roughness rms; correlation length) to two unknowns (dielectric constant; roughness rms)

- calibration involves an optimum roughness correlation length ℓ_{opt}

- this parameter was obtained by forcing the IEM until a good agreement is reached between simulations and SAR image data; calculations were performed using measured rms roughness height and soil moisture content

$$\ell_{opt2} = \delta(sin\theta)^{\mu} rms^{\eta\theta + \xi}$$

$$\delta_{VV} = 3.289$$
$$\delta_{HH} = 4.026$$
$$\xi_{VV} = 1.222$$
$$\xi_{HH} = 1.551$$
$$\eta_{HH} = \eta_{VV} = -0.0025$$
$$\mu_{HH} = \mu_{VV} = -1.744$$

Information source: Baghdadi et al. (2006)

Physical Model: Integral Equation Model

IEM formulation

$$\sigma^o_{pp} = \frac{k^2}{2}\left|f_{pp}\right|^2 exp(-4k^2 s^2 cos^2\theta)\sum_{n=1}^{+\infty}\frac{(4k^2 s^2 cos^2\theta)^n}{n!}W^n(2k\,sin\theta,0)$$

$$+\frac{k^2}{2}Re(f^*_{pp}F_{pp})exp(-3k^2 s^2 cos^2\theta)\sum_{n=1}^{+\infty}\frac{(2k^2 s^2 cos^2\theta)^n}{n!}W^n(2k\,sin\theta,0)$$

$$+\frac{k^2}{8}\left|F_{pp}\right|^2 exp(-2k^2 s^2 cos^2\theta)\sum_{n=1}^{+\infty}\frac{(k^2 s^2 cos^2\theta)^n}{n!}W^n(2k\,sin\theta,0)$$

where

$$f_{hh} = \frac{-2R_h}{cos\theta} \qquad R_h = \frac{cos\theta - \sqrt{\varepsilon_r - sin^2\theta}}{cos\theta + \sqrt{\varepsilon_r - sin^2\theta}} \qquad F_{vv} = -2\frac{sin^2\theta}{cos\theta}\left[\left(1 - \frac{\varepsilon_r cos^2\theta}{\mu_r\varepsilon_r - sin^2\theta}\right)(1-R_v)^2 + \left(1-\frac{1}{\varepsilon_r}\right)(1+R_v)^2\right]$$

$$f_{vv} = \frac{2R_v}{cos\theta} \qquad R_v = \frac{\varepsilon_r cos\theta - \sqrt{\varepsilon_r - sin^2\theta}}{\varepsilon_r cos\theta + \sqrt{\varepsilon_r - sin^2\theta}} \qquad F_{hh} = -2\frac{sin^2\theta}{cos\theta}\left[4R_h - \left(1-\frac{1}{\varepsilon_r}\right)(1+R_h)^2\right]$$

For exponential roughness autocorrelation function

$$W^n(2k\,sin\theta,0) = \left(\frac{\ell}{n}\right)^2\left[1+\left(\frac{2k\ell\,sin\theta}{n}\right)^2\right]^{-1.5}$$

σ^o_{pp} = backscatter at polarization pp (sigma)
θ = incidence angle (radians)
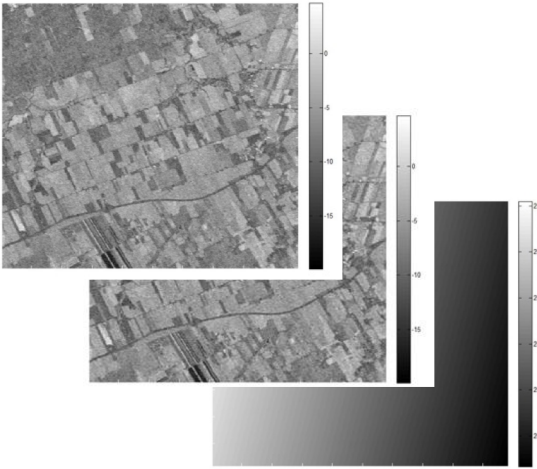ε_r = real part of the dielectric constant
k = is the wave number ($k=2\pi/\lambda$)
s = root mean square height (cm)
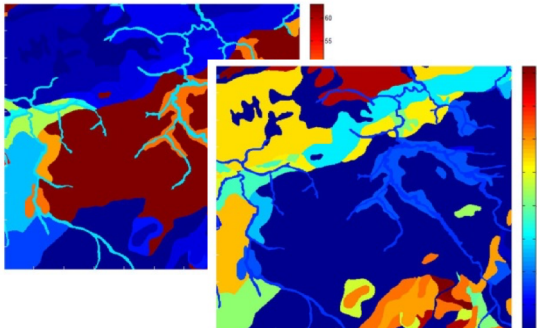ℓ = roughness correlation length (cm)

Physical Modeling Approach
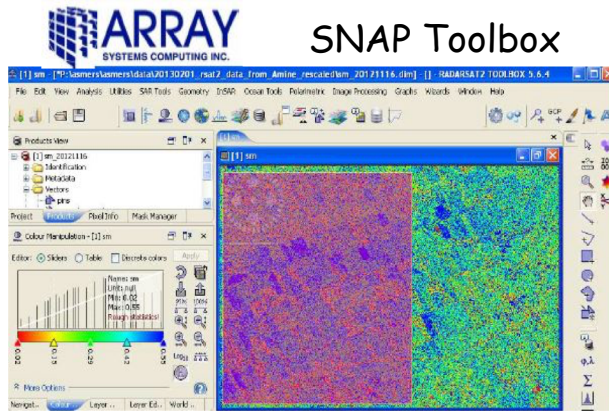
Input Data

Radar Data
(HH and VV Backscatter)
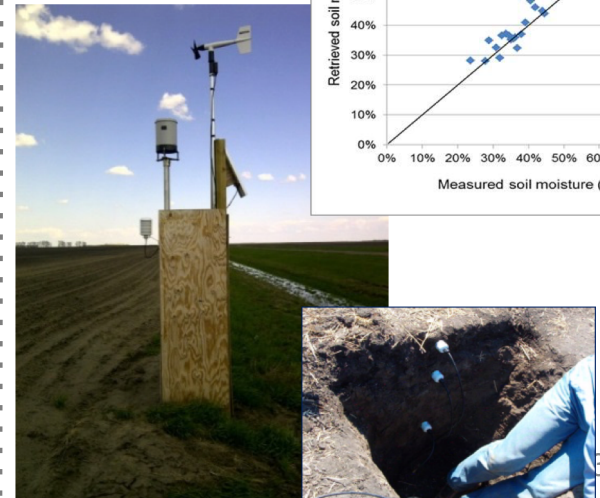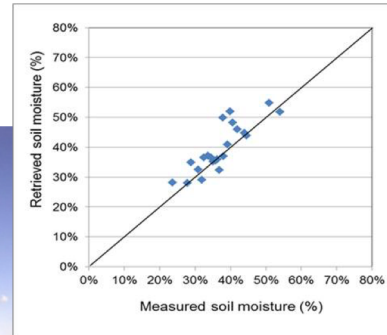(Radar Angle)

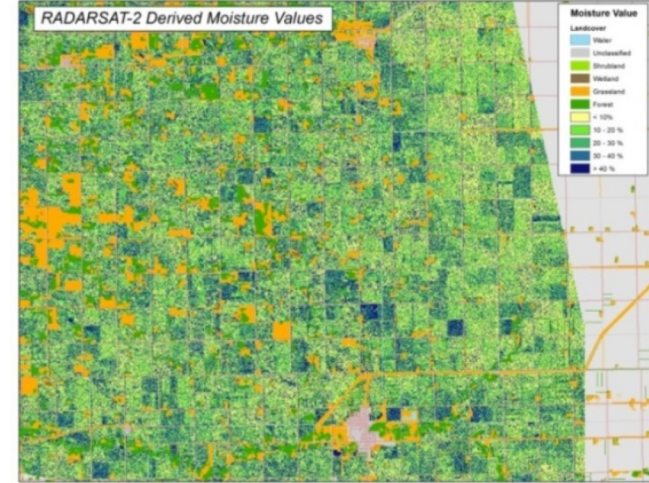Soils Data
(Clay and Sand Fractions)

Data Processing

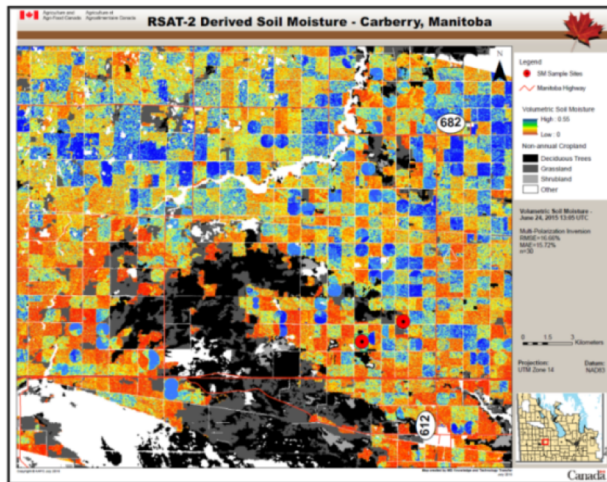IEM with Fresnel Equations
(estimates real dielectric)

SNAP Toolbox

Dielectric Mixing Model
(estimate water fraction
by volume)

Output and Validation

Soil Moisture – Reducing Flood Risk

Percent soil moisture (**wet=blue**)

RSAT-2 Derived Soil Moisture - Carberry, Manitoba

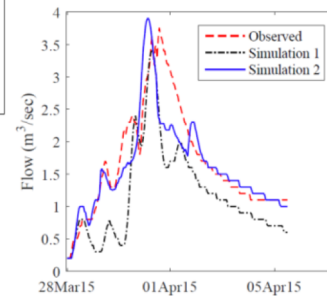**Data**: Canada's RADARSAT-2
Method: physical radar model

2011*: total costs from the Manitoba Flood topped **$1 billion**

2014: Excess moisture insurance payments to farmers who were unable to seed ~**$65 million** (2,400 claims)

Better forecasting means improved early response, mitigation and recovery

WFV — High : 0.55, Low : 0.02
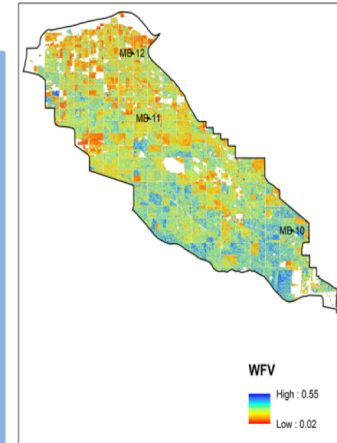
Soil moisture from RADARSAT-2 integrated into hydrological model, improving stream flow forecasts

Precision Irrigation in Chile

Maps of percent soil moisture from RADARSAT-2 (**wet=blue**)

Survival of chicory seedlings depends on adequate access to soil moisture

Dry conditions: 20 October
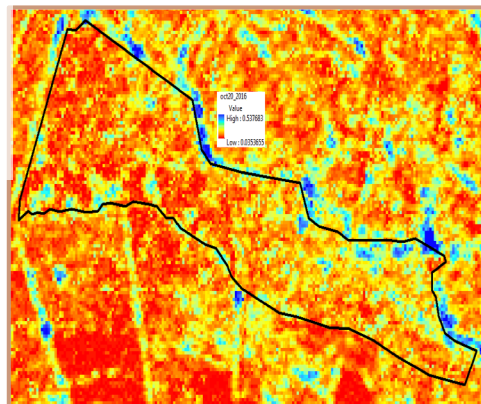
Irrigation occurs: 23 October
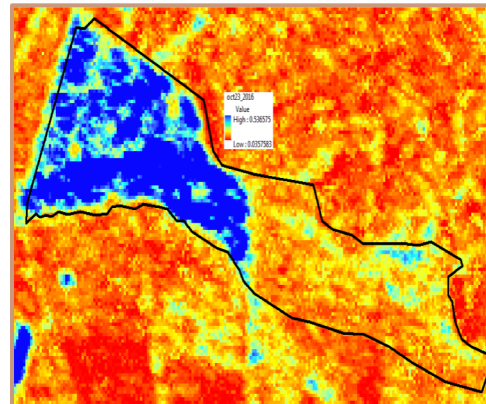
Post-irrigation drying: 30 October

Acknowledgment

Carleton University — Canada's Capital University

Agriculture and Agri-Food Canada — Agriculture et Agroalimentaire Canada

CSA ASC

Natural Resources Canada — Ressources naturelles Canada

PCI Geomatics

Environment and Climate Change Canada — Environnement et Changement climatique Canada

INRS — Institut national de la recherche scientifique

McNairn, H., Shang, J., Jiao, X., and Champagne, C. 2009. The Contribution of ALOS PALSAR Multi-polarization and Polarimetric Data to Crop Classification, IEEE Geoscience and Remote Sensing, 47(12): 3981-3992.

McNairn, H., Kross, A., Lapen, D., Caves, R., and Shang J. 2014. Early season monitoring of corn and soybeans with TerraSAR-X and RADARSAT-2, International Journal of Applied Earth Observation and Geoinformation 28 (2014) 252–259.

Chen, C. and McNairn, H. 2006. A Neural Network Integrated Approach for Rice Crop Monitoring. International J. of Remote Sensing, 26 (7): 1367-1393.

Pei Z, Zhang S, Guo L, McNairn H, Shang J, Jiao X (2011) Rice identification and change detection using TerraSAR-X data. Canadian Journal of Remote Sensing 37:151-156.

Kross, A., Lapen, D.R., McNairn, H., Sunohara, M.D., Champagne, C., and Wilkes, G.A.. "Satellite and in situ derived corn and soybean biomass and leaf area index: response to controlled tile drainage under varying weather condition." 2015, Agricultural Water Management, 160, pp. 118-131.

Hosseini, M., McNairn, H., Merzouki, A., and Pacheco, A., "Estimation of Leaf Area Index (LAI) in corn and soybeans using multi-polarization C- and L-band radar data", Remote Sensing of Environment, vo. 170, pp. 77-89, 1 December 2015.

McNairn, H., Jiao, X., Pacheco, A., Sinha, A., Tan, W., and Li, Y. (2018). Estimating canola phenology using synthetic aperture radar, Remote Sensing of Environment, 219: 196-205.

P. C. Dubois, J. Van Zyl, and T. Engman, "Measuring soil moisture with imaging radars," *IEEE Trans. Geosci. Remote Sens.*, vol. 33, no. 6, pp. 915–926, Nov. 1995.

Y. Oh, K. Sarabandi, and F. T. Ulaby, "An empirical model and an inversion technique for radar scattering from bare soil surfaces," *IEEE Trans. Geosci. Remote Sens.*, vol. 30, no. 2, pp. 370–381, Mar. 1992.

A.K. Fung, Z. Lee, and K. S. Chen, "Backscatter from a randomly rough dielectric surface," IEEE Trans. Geosci. Remote Sens., vol. 30, no. 2, pp. 356-369, Mar. 1992.

N. Baghdadi, N. Hola, and M. Zribi, "Calibration of the integral equation model for SAR data in C-band and HH and VV polarizations," *Int. J. Remote Sens.*, vol. 27, no. 4, pp. 805–816, Feb. 2006.